Large Dynamic Range Optical Fiber Distributed Acoustic Sensing (DAS) With Differential-Unwrapping-Integral Algorithm

Fan Cunzheng, Li Hao, He Tao, Zhang Shixiong, Yan Baoqiang, Yan Zhijun, and Sun Qizhen, *Senior Member, IEEE*

***Abstract*—Optical fiber distributed acoustic sensing (DAS) based on phase sensitive optical time domain reflectometry (φ-OTDR) has a great demand in many application fields with large signals, such as railway safety monitoring, cable vibration detection, etc. However, due to the inherent limits of phase unwrapping algorithm, the large signal whose phase change exceeds π cannot be recovered correctly by DAS. In this work, the differential-unwrapping-integral (DUI) algorithm is proposed and demonstrated to replace the traditional unwrapping algorithm for large signal recovery. By utilizing differential operation to compress the signal amplitude, the large phase signal can be converted into small signal which can be recovered through unwrapping. Then, multiple integral operations and polynomial fitting compensation algorithm are applied onto the differential signal to recover the original phase signal without any signal-to-noise ratio(SNR) sacrificed. In theory, the maximum measurable phase of DUI can be improved 1390 times compared with traditional DUI algorithm. Further, the experimental results demonstrate that the dynamic range of DAS with DUI can reach up to 131.7 dB. Moreover, DUI algorithm has been tested and verified in the field test for recording the digging signals with large amplitude. This scheme can be applicable for all phase-demodulation-based sensing techniques without increasing the system complexity.**

***Index Terms*—Large dynamic range measurement, optical fiber distributed acoustic sensing, phase demodulation.**

I. Introduction

DUE to the advantages of ultra-high sensitive, long-distance passive measurement and the immunity to EMI, the demand for distributed acoustic sensing (DAS) technology based on phase sensitive optical time domain reflectometry (φ-OTDR) is growing in many areas recently [1]–[4]. Many researchers have studied phase extraction methods for φ-OTDR such as 3 $\times$ 3 coupler method [5], phase-generated carrier(PGC) method [6], TGD-OFDR method [7] and digital coherent demodulation [8]–[10]. However, most of the methods demodulate the phase through the inverse trigonometric operation and unwrapping algorithm, which can only recover signals whose phase change between adjacent sampling points is less than π rad [11]. The π-phase constraint limits the applications of DAS in special fields with large signals, such as railway safety monitoring, pipeline detection and underwater acoustic sensing.

Several techniques have been reported to enlarge the dynamic range of strain sensing. In the dual-wavelength method [12], two probe pulses with different wavelengths were injected into the sensing fiber simultaneously and the phase difference between two wavelengths was used for phase extraction. Since the phase difference is much smaller than the phase of single wavelength, 24.08 $\mu\varepsilon$ strain signals was recovered by unwrapping the phase difference. Because the signal is reduced while the noise stays at the same level, the SNR is deteriorated definitely. In addition, the system complexity increases greatly. Besides, some DAS systems relying on measuring the backscattered amplitude can also improve the dynamic range [13], [14], such as the chirped-pulse phase-sensitive OTDR technology. Through emitting the chirped-pulse into sensing fiber and transforming the phase change into the time delay, the π-phase constraint was broken successfully, which could demodulate the large signal with a 65 $\mu\varepsilon$ amplitude [15]. However, the method needs the complex pulse modulation and high speed data acquisition to increase SNR, which has a high hardware cost.

In this work, a differential-unwrapping-integral (DUI) algorithm was proposed for realizing large dynamic range in φ-OTDR based DAS system [16]. Since differential operation depresses the amplitude of signals, the acoustic signals whose phase changes between adjacent sampling points exceed π can be unwrapped correctly by choosing appropriate differential order. Then, through multiple integral operations and polynomial fitting compensation algorithm, the original phase can be recovered without any additive noise or extra device cost. The DUI theoretical model was presented to analyze the influence factor of dynamic range. Furthermore, a coherent detection based DAS system with DUI algorithm was established. The maximum phase of 1043rad (i.e., 387 $\mu\varepsilon$) at the frequency of 1.08 kHz was

Manuscript received June 29, 2021; revised August 19, 2021; accepted September 3, 2021. Date of publication September 8, 2021; date of current version November 16, 2021. This work was supported in part by the National Key Research and Development Program of China under Grant 2018YFB2100902, in part by the National Natural Science Foundation of China (NSFC) under Grants 61922033 and 61775072, in part by the quick response project of National Defense Science and Technology Innovation under Grant 20-163-00-KX-001-014-02, in part by the Fundamental Research Funds for the Central Universities HUST:2021JYCXJJ036, and in part by the Innovation Fund of WNLO. *(Corresponding author: Qizhen Sun.)*

The authors are with the School of Optical and Electronic Information, Wuhan National Laboratory for Optoelectronics, National Engineering Laboratory for Next Generation Internet Access System, Huazhong University of Science and Technology, Wuhan, Hubei 430074, China (e-mail: buckt@hust.edu.cn; lhbeyond@hust.edu.cn; walnut@hust.edu.cn; zhangshixiong@hust.edu.cn; yanbaoqiang@hust.edu.cn; yanzhijun@hust.edu.cn; qzsun@mail.hust.edu.cn).

Color versions of one or more figures in this article are available at https://doi.org/10.1109/JLT.2021.3110768.

Digital Object Identifier 10.1109/JLT.2021.3110768

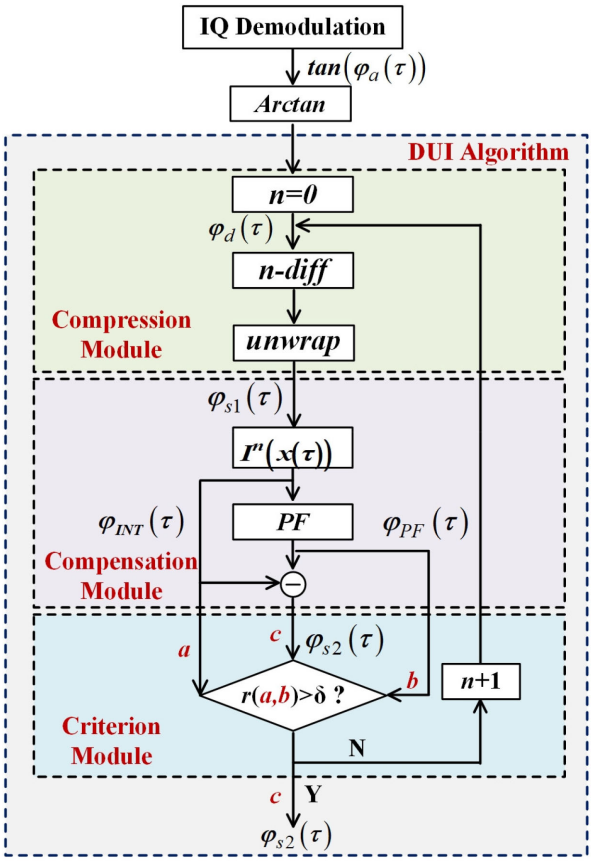

Fig. 1. The processing flow of DUI algorithm. $\varphi_a(\tau)$: The actual phase signal; $\varphi_d(\tau)$: The demodulated phase signal; $\Delta^n \mathrm{x}(\tau)$: nth differential operation, $\Delta^n \mathrm{x}(\tau) = \Delta^{n-1}(\mathrm{x}(\tau) - \mathrm{x}(\tau-1))$; $\varphi_{S1}(\tau)$: The output of Compression Module; $I^n \mathrm{x}(\tau)$: nth integral operation, $I^n \mathrm{x}(\tau) = I^{n-1}(\sum_1^\tau x(\tau))$; $\varphi_{INT}(\tau)$: The output of integral operation; PF: Polynomial fitting; $\varphi_{PF}(\tau)$: The output of PF operation; $\varphi_{S2}(\tau)$: The output of Compensation Module; r(a,b): correlation coefficient between sequence a and sequence b. .

successfully recovered with high accuracy, corresponding to the large dynamic range over 131 dB. Moreover, DUI algorithm has been used in the field test, whose availability in the field was tested and verified.

II. Principle

A. DUI Phase Demodulation Algorithm

The flow chart of the DUI algorithm is illustrated in Fig. 1(a), which contains compression module, compensation module and criterion module. For simplicity, assuming that the original signal is a single frequency harmonic vibration defined as $\varphi_a\ (t) = \ Asin(2\pi ft + \theta)$, where A is the amplitude, f is the signal frequency and θ is the initial phase with a random constant ranging from 0 to 2π. If the sampling rate of DAS is f_s, φ is sampled as $\varphi_a\ (\tau) = \ Asin(2\pi f\tau/f_s + \theta)$, where τ is the sampling ordinal.

Firstly, the compression Module is performed after IQ demodulation [17], and arctangent operation. Because the arctangent operation will wrap $\varphi_a(\tau)$ into a phase period, the output $\varphi_{\mathrm{d}}\ (\tau) = \varphi_{\mathrm{a}}\ (\tau) + 2\mathrm{k}(\tau)\pi$ where $-\pi < \varphi_{\mathrm{d}}(\tau) \leq \pi$ and $\mathrm{k}(\tau)$ are integers. Through n^{th} differential operation, the signal can be expressed as

$$\Delta^n \varphi_d\ (\tau) = \Delta^n \varphi_a\ (\tau) + 2\pi \cdot \Delta^n k\ (\tau) \tag{1}$$

where $\Delta^n \varphi_a\ \ (\tau) = \gamma^n\ \ Asin(2\pi f\tau/f_s + \theta + n\theta')$, $\gamma\ = \ 2sin(\pi f/f_s)$ is the amplitude coefficient and $\theta' = \ -\pi f/f_s + 0.5\pi$ is phase coefficient. Obviously, when $f_s/f > 6$, amplitude coefficient γ will be less than 1, which indicates the amplitude of actual phase signal can be depressed. Mathematically, through multiple differential, $|\Delta(\Delta^n \varphi_a(\tau))|$ will be compressed within π, so that $\Delta^n \varphi_a(\tau)$ can be recovered successfully by unwrapping operation from $\Delta^n \varphi_d(\tau)$. After unwrapping, the differential signal is sent to Compensation Module.

In the following Compensation Module, the actual phase signal $\varphi_a(\tau)$ is recovered from $\varphi_{S1}(\tau)$. Firstly, the integral operation is adopted, obtaining the phase signal $\varphi_{INT}(\tau)$. While, the nth order polynomial error $\varphi_{PE}(\tau)$ is also introduced, which is described as

$$\varphi_{INT}\ (\tau) = \varphi_a\ (\tau) + \sum_{i=0}^{n} \tau^i z_i = \varphi_a\ (\tau) + \varphi_{\mathrm{PE}}\ (\tau) \tag{2}$$

where the error coefficients are $\mathrm{z}_i = \ -\Delta^i \varphi_a(0)(\mathrm{when\ i} < \mathrm{n})$ $and\ \ \mathrm{z}_n = \ 2\pi \cdot \Delta^n k(0)$. For the rapidly changing signal, the actual signal $\varphi_a(\tau)$ has a finite amplitude and fluctuates over time. In the polynomial fitting step, $\varphi_{INT}(\tau)$ is fitted to a polynomial through least square method for estimating $\varphi_{PE}(\tau)$. However, the actual signal $\varphi_a(\tau)$ is a disturbance signal with arbitrary type, and hence this fitting process will bring the phase error to polynomial fitting result $\varphi_{PF}(\tau)$. As we all know, the least square method can estimate target parameter from disturbance signal with a finite amplitude, and it will be more accurate when sequence length is longer [18]. Therefore, if the signal sequence for recovery is long enough in time domain, the disturbance of $\varphi_a(\tau)$ can be ignored, and the PF operation can estimate $\varphi_{PE}(\tau)$ with great accuracy i.e., $\varphi_{PF}\ (\tau) = \varphi_{PE}\ (\tau)$. Hence, the final result $\varphi_{s2}(\tau)$ can be regarded as the same with the actual signal $\varphi_a(\tau)$ as follows:

$$\varphi_{s2}\ (\tau) = \varphi_{INT}\ (\tau) - \varphi_{PF}\ (\tau) = \varphi_a\ (\tau) \tag{3}$$

Then, the output $\varphi_{S2}(\tau)$ is sent to Criterion Module to judge whether the actual phase signal is recovered successfully. The similarity degree between the output of integral operation $\varphi_{INT}(\tau)$ and the output of PF $\varphi_{PF}(\tau)$ is served as the criterion skillfully, which can be expressed as

$$r\ (\varphi_{INT}\ (\tau), \varphi_{PF}\ (\tau)) \geq \delta \tag{4}$$

where δ is adjustable with the optimized value of 0.99999999 and r is the correlation coefficient defined as

$$r\ (a, b)\ = \sum_{i=1}^{m} (a_i - \overline{a})\ (b_i - b) \Big/ \sqrt{\sum_{i=1}^{m} (a_i - \overline{a})^2 \cdot \sum_{i=1}^{m} (b_i - \overline{b})^2} \tag{5}$$

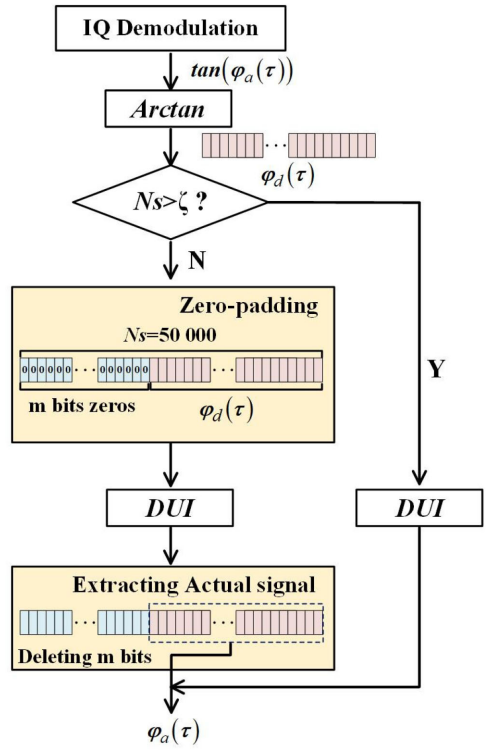

Fig. 2. The processing flow of zero-padding.

If the actual phase signal is recovered successfully, $\varphi_{INT}(\tau)$ and $\varphi_{PF}(\tau)$ are very similar, and the similarity degree will be larger than 0.99999999. However, if the differential order n is not large enough, the integral error is a piecewise polynomial, which cannot be fitted by PF. So the similarity degree between $\varphi_{INT}(\tau)$ and $\varphi_{PF}(\tau)$ is less than 0.99999999 definitely. Therefore, if (3) is satisfied, it means that $\varphi_a(\tau)$ is recovered successfully by DUI, otherwise $(\mathrm{n}+1)^{\mathrm{th}}$ DUI algorithm needs to be conducted. Specially, the traditional unwrapping operation can be regarded as the 0th-order DUI.

According to above discussion, a long enough signal sequence is needed for recovering signal with a negligible noise. Therefore, for a short signal, the length of signal sequence Ns need to be extended. In practice, the zero-padding method is used for extending the length, whose processing flow is shown in Fig. 2. Firstly, the length of signal Ns is compared with the target length ζ, where ζ is adjustable with the optimized value of 50 000. If Ns is lower than 50 000, the arctangent signal $\varphi_d(\tau)$ will be extended to 50 000 through adding m bits zeros in the front of signal. Then, the splicing signal is sent to DUI algorithm, where the signal will be recovered with a negligible noise. After that, the actual signal is extracted out from the output of DUI through deleting the front m bits.

B. Maximum Measurable Amplitude of DUI

Based on the above analysis, the π-phase constraint in n^{th} DUI algorithm is $|\Delta^{n+1}\varphi(\tau)| \leq \pi$, and thus the amplitude of signal A needs to satisfy $\gamma^{n+1}A \leq \pi$. While the phase constraint in traditional unwrapping is $|\Delta\varphi(\tau)|_{max} \leq \pi$ and the maximum measurable amplitude(MMA) need to satisfy $\gamma A \leq \pi$. Compared with the traditional unwrapping algorithm, MMA of n^{th} DUI algorithm can be greatly increased as

$$\beta = 1/\gamma^n \tag{6}$$

under the condition of $f_s/f > 6$, where $\gamma = 2sin(\pi f/f_s)$.

Further, the performance of DUI algorithm is theoretically investigated, where the phase noise with a Gaussian distribution is taken into the consideration. We assume the phase to be extracted is $\varphi(\tau) = Asin(2\pi f\tau/f_s + \theta) + n_p(\tau)$, where $n_p(\tau)N(0, {\sigma_p}^2)$ is the noise, $\sigma_p$is the standard deviation. Then the phase constraints of DUI algorithm should be modified as

$$\gamma^{n+1}A + 2|\Delta^n n_p(\tau)|_{\max} \leq \pi \tag{7}$$

As we all know, the empirical rule predicts that 99.7% of Gaussian noise value is within the first three standard deviations ($\mu \pm 3\sigma$)". Therefore, the value range of $n_p(\tau)$ can be expressed as $[-3\sigma_p, 3\sigma_p]$ and then the phase constraint of traditional unwrapping method can be expressed as $\gamma A + 6\sigma_p \leq \pi$. Furthermore, we defined the noise figure $X(n)$ as $\Delta^n n_p(\tau)_{max}/n_p(\tau)_{max}$, so that the value ranges of $\Delta^n n_p(\tau)$ are $[-3X(n)\sigma_p, 3X(n)\sigma_p]$ and the phase constraints of DUI can be corrected as

$$\gamma^{n+1}A + 6\mathrm{X}(\mathrm{n})\,\sigma_{\mathrm{p}} \leq \pi. \tag{8}$$

Equation (8) indicates that the differential order n is limited by the phase noises. With the increase of differential order, the noise level is increased rapidly. When the noise reaches π, the phase signals cannot be recovered. if the standard deviation of noise σ_p, the order of DUI n and frequency sample f_s are kept constant, when the phase amplitude increase m times, frequency response of DUI need decrease $\sqrt[n+1]{\mathrm{m}}$ times to recover the phase signal. However, the limit of frequency response can be improved greatly when the noise level is reduced since a lower noise can support a larger DUI order n.

It need to be noted that DUI is also suitable for multi-frequency signals, whose phase constraints of DUI can be corrected as

$$\int_{f_1}^{f_2} \gamma(f)^{\mathrm{n}+1} A(f) + 6\mathrm{X}(\mathrm{n})\,\sigma_{\mathrm{p}} \leq \pi \tag{9}$$

where $[f_1, f_2]$ is the signal frequency distribution. What's more, when $f_s/f < 6$, the DUI degenerates into the unwrapping operation (i.e., 0th order DUI), whose MMA will be same as the traditional unwrapping method.

Moreover, we systematically analyze the impact of the phase noises σ_p, differential number n and sampling frequency f_s on MMA in theory. The 1 kHz sine signals with different amplitude are modulated on optical phases as an example. The sampling rate is set as 50 kHz, and the change of MMA with noise variance from $10^{-6}rad^2$ to $10^{-1}rad^2$ and differential number n ranging from 1 to 5 is analyzed, as drawn in Fig. 3(a). It can be seen that compared with the traditional unwrapping algorithm, MMA of a higher order DUI have a greater improvement under a proper noise condition. For example, when the noise variance is -30 dB *re* rad^2, the MMA can be improved 1390 times. Further, we set the sampling rate from 6 kHz to 50 kHz. The dependence of

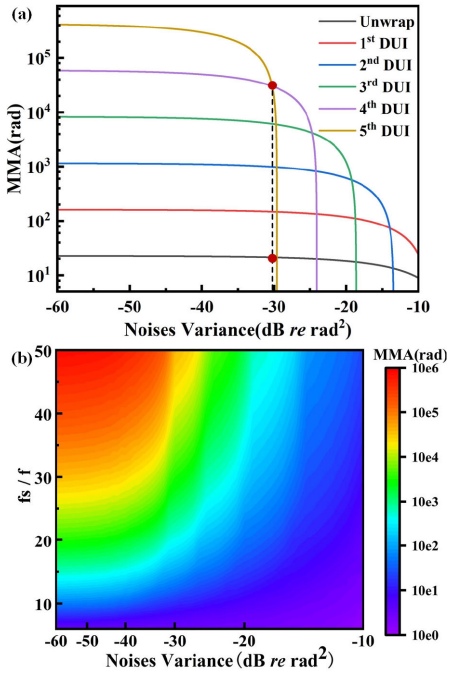

Fig. 3. (a) The relationship between MMA and noise variance with different differential number when f_s/f is 50 kHz. (b) MMA distribution with noise variance and f_s/f.

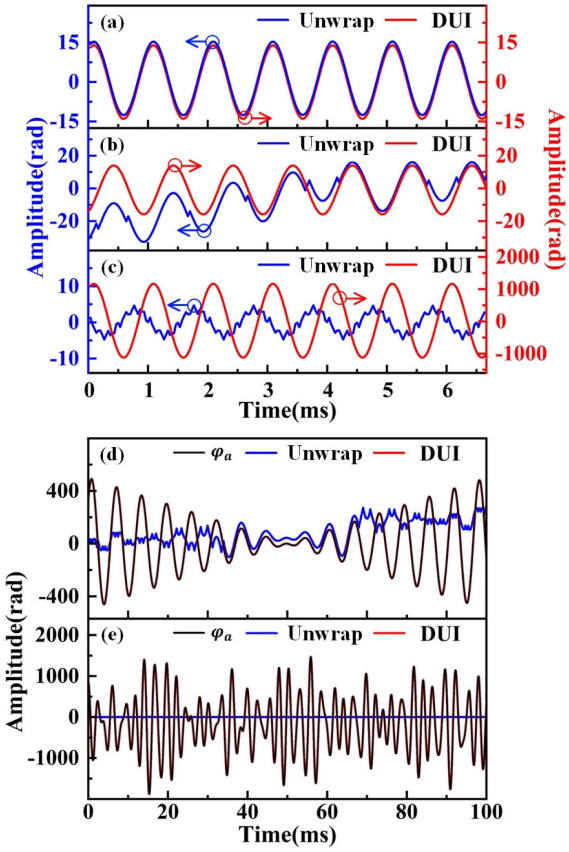

Fig. 4. Simulation results. Time domain signals when amplitude is (a) 14rad, (b) 15rad and (c) 1150rad. (d)(e) Multi-frequency signal.

MMA on noise level and sampling rate are illustrated in Fig. 3(b) It is clear that MMA at optimized n is increased with higher sample rating and lower noise level.

Furthermore, the recovery performances of DUI algorithm for different types of signals are analyzed. Firstly, a 1 kHz sine signal with 10^{-3} rad^2 noise variance is modulated on optical phases, and the sampling rate is set at 30 kHz. When the amplitude of the phase signal is changed from 1rad to 1200rad, the recovery results of 3rd DUI algorithm at typical amplitude of 14rad, 15rad and 1150rad are illustrated in Figs. 4(a)–4(c). Notably, the demodulation results of traditional unwrapping algorithm are also plotted for comparison. It can be seen that the traditional unwrapping algorithm can only recover the signal with amplitude less than 14rad, while the MMA of DUI algorithm can reach 1150rad. What's more, complex signals such as the harmonic signal with a triangular envelope and multiple frequencies signal can also be recovered successfully by DUI method, which are presented in Figs. 4(d)–(e).

III. Experiment and Result

A. Laboratory Experiment

To verify the theoretical analysis above, the experimental demonstration is developed with the DAS system configuration as shown in Fig. 5. Coherent detection and polarization diversity reception are employed for a higher signal-to-noise ratio (SNR). The CW light from Narrow linewidth laser(NLL) is split into two beams by an 1×2 optical coupler (OC1). The local light is split into two beams by an 1×2 optical coupler (OC2). The probe light is injected into an acousto-optic modulator (AOM) to generate optical pulses with 200 MHz frequency shift and 50ns pulse duration. After amplified by the erbium-doped optical fiber amplifier (EDFA), the probe pulses are transmitted into the fiber under test (FUT).In the FUT, the discrete scattering enhanced points are inscribed along the fiber through UV exposure to eliminate the interference fading [19], and the interval of the adjacent scattering points is selected as 20m to obtain a larger amplitude phase signal. The near-end of FUT is wrapped around a piezoelectric transducer (PZT) while the far-end of FUT is stuck to the vibration table (VT) to excite acoustic waves. At the receiver end, backscattered light of probe pulses is split into two orthogonal polarization beams. Then each polarization beam and a split local light are mixed in the 2×2 couplers (OC3, OC4), respectively. After that, the outputs are converted into electrical signal by balanced photodetectors (BPD). Then, IQ demodulation [17] and the rotated-vector-sum method [20] were used to demodulate and combine information measured in the two polarization states. Finally, the signals were recovered by DUI algorithm.

Firstly, the demodulation signals and noise of unwrapping operation and DUI algorithm are compared through the PZT vibration. We set the sampling frequency of DAS at 5 kHz and the PZT is driven by a 250 Hz sinusoidal wave with adjustable peak-to-peak voltage Vpp. Figs. 6(a)-6(c) depict the recovery results of different algorithms when Vpp are 78V, 120V and

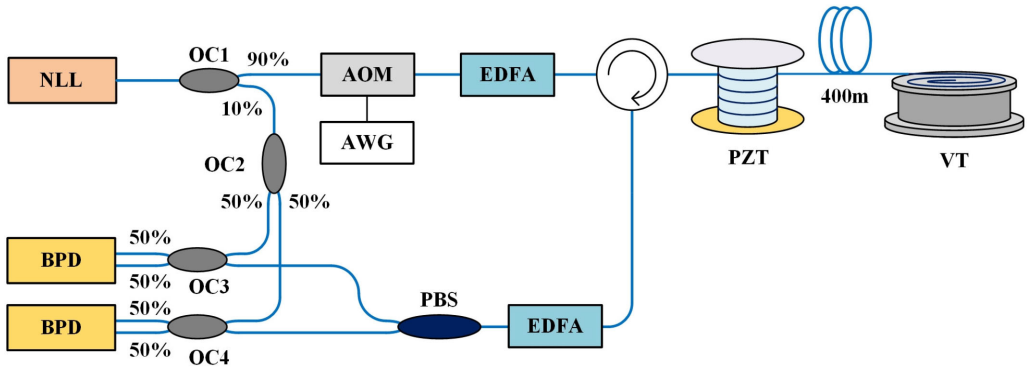

Fig. 5. The configuration of experimental setup.

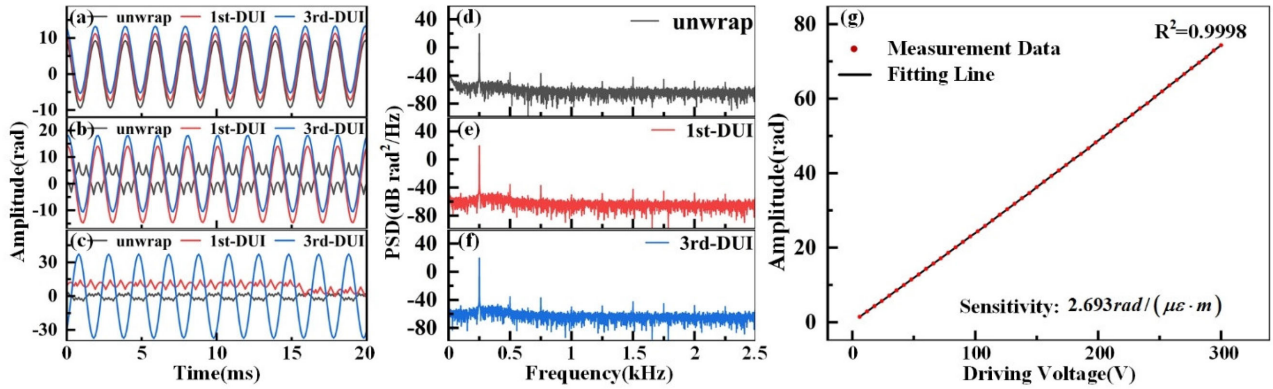

Fig. 6. Recovered 250 Hz phase signals with the driving voltage of (a) 78V, (b) 120V, (c) 300V. PSD of (a). PSD of 250 Hz signals with the driving voltage of 78V recovered by (d) unwrapping algorithm, (e) 1st-order-DUI algorithm and (f) 3rd-order-DUI algorithm. (g) The relationship between the PZT driving voltage and the amplitude of the demodulated phase.

300V, respectively. It can be seen that the unwrapping operation can only recover 18.6rad signals, while the DUI algorithm can recover larger signals, and the higher order of DUI algorithm, the larger MMA. What's more, as shown in Figs. 6(d)-6(f), the power spectra of signals recovered by unwrapping and DUI algorithm are almost identical, in which harmonic peaks are caused by the nonideal PZT incentive. [21]The result experimentally proves that the DUI algorithm can recover signals without SNR deterioration. Then, the strain sensitivity calibrated by the DUI algorithm is investigated. As shown in Fig. 6(g), the voltage-strain conversion relationship of PZT is $0.0092\mu\varepsilon/V$, and consequently the DUI algorithm has a great linear strain response with strain sensitivity of $2.693rad/(\mu\varepsilon \cdot m)$ and R2 = 0.9998.

Secondly, dynamic strain of DUI is experimentally verified. The sampling frequency of DAS is set as 50 kHz and the VT is driven by a 1.08 kHz sinusoidal wave with adjustable peak-to-peak voltage from 10mV to 1900mV to provide extra-large signal. The traditional unwrapping operation only can recover dynamic strain signal with 48.98rad amplitude. As demonstrated in Fig. 7(a), the DUI algorithm can recover dynamic strain signal with 1043rad amplitude and 1900mV driving Vpp, corresponding to a large strain up to $387\mu\varepsilon$. It should be noted that the signal is the largest strain that can be generated by this VT. To

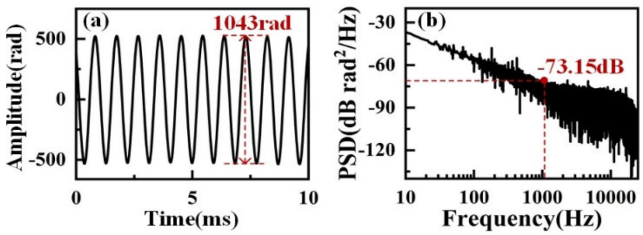

Fig. 7. (a) Signal recovered by 3rd DUI. (b) PSD in quiet environment.

evaluate the enhancement effect of dynamic range, the results in quiet environment with the same condition is sensed and demodulated, whose PSD is plotted in Fig. 7(b). The noise floor at 1.08 kHz is -73.15 dB for a frequency resolution of 1 Hz, corresponding to a small strain of only $100.3p\varepsilon$. Therefore, the dynamic ranges of DUI and standard unwrapping operation are respectively 131.7 dB and 105.1 dB, demonstrating a 26.6 dB improvement of DUI.

Furthermore, PZT and VT are driven by sinusoidal wave with the frequencies of 6 kHz and 1.08 kHz respectively, to generate two signals at different sections simultaneously. The sampling frequency is set as 50 kHz. Fig. 8(a) shows the acoustic waves

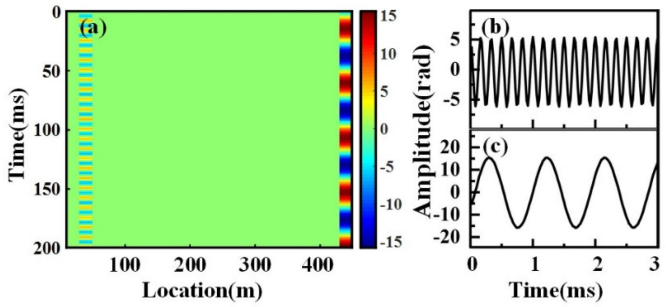

Fig. 8. (a) Spatial and temporal distribution of acoustic waves demodulated by DUI; acoustic waves exerted by (b) PZT and (c) VT.

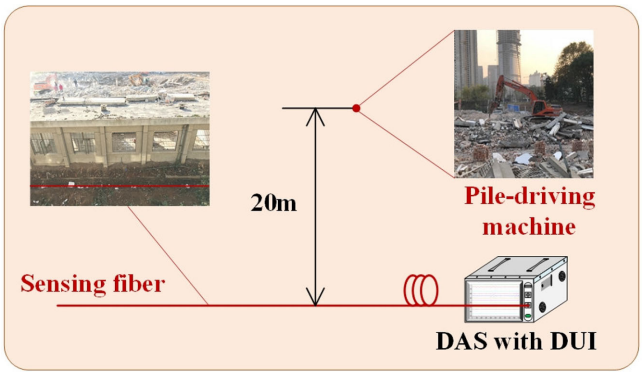

Fig. 9. Engineering application environment.

in each sensing channel with 20m spacing, and the demodulated acoustic waves of two sensing channels at PZT and VT are presented in Figs. 8(b) and 8(c), respectively. As expected, the two acoustic waves are successfully recovered by DUI algorithm, which proves that DUI algorithm has the ability of distributed detection.

It should be noted that the DUI algorithm will not introduce additional noise compared with the traditional method. Although the noise will be increased in the differential process, integral operation will completely restore the noise to its original intensity. In addition, owing that the DUI algorithm is adopted after arctangent operation of phase demodulation, it can be utilized by all phase-demodulation-based sensing techniques to extent the dynamic range without any additive noise or extra device cost.

B. Field Test

The DUI algorithm has been tested and verified in practical applications. Here is a field test of perimeter security. As shown in Fig. 9, the sensing fiber is buried in the soil to measure the acoustic signal from various construction events with 5 m channel spacing and a pile-driving machine worked at 20 m from optical fiber.

Firstly, the pile-driving signals are detected with a higher sampling frequency of 10 kHz, which can be correctly recovered by traditional unwrapping operation. And the recovered signal is served as the original signal. Then, the collected signal is

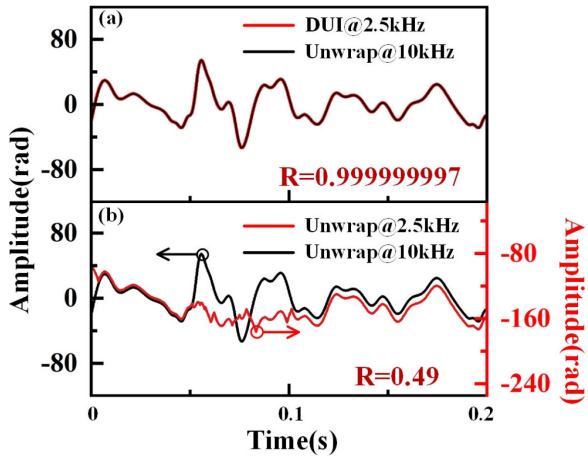

Fig. 10. Acoustic signals of Single pile-driving. (a) Demodulated by unwrapping operation with 10 kHz sampling rate and DUI algorithm with 2.5 kHz sampling rate, respectively. (b) Demodulated by unwrapping operation with the sampling rates of 10 kHz and 2.5 kHz, respectively.

downsampled from 10 kHz to 2.5 kHz, and further demodulated by traditional unwrapping operation and DUI algorithm, respectively. From the results shown in Fig. 10, the DUI algorithm can recover the signal with an ultra-high accuracy, whose correlation coefficient R with the original signal can reach 0.999999997. However, the traditional unwrapping operation cannot recover the signal correctly, with a correlation coefficient R of only 0.49. The field test results show that the DUI algorithm can precisely recover the dynamic signal with large amplitude.

IV. Conclusion

In this work, a DUI algorithm is proposed and verified for expanding the dynamic range of DAS. Theoretical analysis shows that the dynamic range of DUI is increased by the increase of sampling frequency and differential order. 1.08 kHz sinusoidal wave with phase amplitude of $387\mu\varepsilon$ strain is demodulated by DUI algorithm without sacrificing any SNR. Significantly, the dynamic range is greatly improved to over 131 dB at the frequency of 1.08 kHz. The algorithm also exhibits the capabilities of linear response and distributed detection, and it has been tested and verified in the field test. Furthermore, the DUI algorithm is universal for all the phase demodulation techniques including 3×3 coupler method, phase-generated carrier(PGC) method, TGD-OFDR and their improved methods. The DUI algorithm greatly expand the application scope of DAS, especially in the fields requiring large signal measurement such as railway monitoring and tunnel safety monitoring.

References

[1] H. Li, T. Liu, D. Liu, Z. Yan, and Q. Sun, "SNR improvement of distributed acoustic sensing through optimizing gauge length," in *Proc. IEEE Asia Commun. Photon. Conf. (ACP)*, 2019, pp. 1–3.

[2] H. Li *et al.*, "Ultra-High sensitive quasi-distributed acoustic sensor based on coherent OTDR and cylindrical transducer," *J. Lightw. Technol.*, vol. 38, no. 4, pp. 929–938, 2020.

[3] H. Liu, J. Ma, T. Xu, W. Yan, and X. Zhang, "Vehicle detection and classification using distributed fiber optic acoustic sensing," *IEEE Trans. Veh. Technol.,* vol. 89, no. 2, pp. 1363–1374, Feb. 2020.
[4] T. Liu *et al.*, "Ultra-high resolution strain sensor network assisted with an LS-SVM based hysteresis model," *Opto-Electron. Adv.,* vol. 4, no. 5, pp. 200037–1–200037–11, 2021.
[5] X. Zhang *et al.*, "A high performance distributed optical fiber sensor based on Φ-OTDR for dynamic strain measurement," *IEEE Photon. J.,* vol. 9, no. 3, Jun. 2017, Art. no. 6802412.
[6] G. Fang, T. Xu, S. Feng, and L. Fang, "Phase-Sensitive optical time domain reflectometer based on phase-generated carrier algorithm," *J. Lightw. Technol.,* vol. 33, no. 13, pp. 2811–2816, 2015.
[7] D. Chen, Q. Liu, X. Fan, and Z. He, "Distributed fiber-optic acoustic sensor with enhanced response bandwidth and high signal-to-noise ratio," *J. Lightw. Technol.,* vol. 35, no. 10, pp. 2037–2043, 2017.
[8] H. He *et al.*, "SNR enhancement in phase-sensitive OTDR with adaptive 2-D bilateral filtering algorithm," *IEEE Photon. J.,* vol. 9, no. 3, Jun. 2017, Art. no. 6802610.
[9] Y. Quan *et al.*, "Compensating for influence of laser-frequency-drift in phase-sensitive OTDR with twice differential method," *Opt. Exp.,* vol. 27, no. 3, pp. 3664–3671, 2019.
[10] J. Wang *et al.*, "Diaphragm-based optical fiber sensor array for multipoint acoustic detection," *Opt. Exp.,* vol. 26, no. 19, pp. 25293–25304, 2018.
[11] K. Itoh, "Analysis of the phase unwrapping algorithm," *Appl. Opt.,* vol. 21, no. 14, 1982, Art. no. 2470.
[12] H. He, L. Yan, H. Qian, X. Zhang, B. Luo, and W. Pan, "Enhanced range of the dynamic strain measurement in phase-sensitive OTDR with tunable sensitivity," *Opt. Exp.,* vol. 28, no. 1, pp. 226–237, 2020.
[13] M. Fernández-Ruiz, L. Costa, and H. F. Martins, "Distributed acoustic sensing using chirped-pulse phase-sensitive OTDR technology," *Sensors,* vol. 19, no. 20, pp. 4368–4395, 2019.
[14] D. Chen, Q. Liu, Y. Wang, H. Li, and Z. He, "Fiber-optic distributed acoustic sensor based on a chirped pulse and a non-matched filter," *Opt. Exp.,* vol. 27, no. 20, pp. 29415–29424, 2019.
[15] J. Zhang *et al.*, "Extending the dynamic strain sensing rang of phase-OTDR with frequency modulation pulse and frequency interrogation," 2019. *arXiv :1911.10468* .
[16] C. Fan, H. Li, T. Liu, Z. Yan, and Q. Sun, "DUI algorithm for improving the dynamic range of fiber optic distributed acoustic sensor," in *Proc. Asia Commun. Photon. Conf.*, 2020, Art. no. S4G.5.
[17] F. Wang *et al.*, "Polarization fading elimination for ultra-weak FBG array-based Φ-OTDR using a composite double probe pulse approach," *Opt. Exp.,* vol. 27, no. 15, pp. 20468–20478, 2019.
[18] J. L. Devore, K. N. Berk, and M. A. Carlton, *Modern Mathematical Statistics With Applications*. Berlin, Germany: Springer, 2012.
[19] B. Redding, M. J. Murray, A. Donko, M. Beresna, and G. Brambilla, "Low-noise distributed acoustic sensing using enhanced backscattering fiber with ultra-low-loss point reflectors," *Opt. Exp.,* vol. 28, no. 10, pp. 14638–14647, 2020.
[20] D. Chen, Q. Liu, and Z. He, "Phase-detection distributed fiber-optic vibration sensor without fading-noise based on time-gated digital OFDR," *Opt. Exp.,* vol. 25, no. 7, 2017, Art. no. 8315.
[21] Habibullah, H. R. Pota, I. R. Petersen, and M. S. Rana, "Creep, hysteresis, and cross-coupling reduction in the high-precision positioning of the piezoelectric scanner stage of an atomic force microscope," *IEEE Trans. Nanotechnol.,* vol. 12, no. 6, pp. 1125–1134, Nov. 2013.

Cunzheng Fan received the B.S. degree in 2018 in optoelectronics information science and engineering from the Huazhong University of Science and Technology, Wuhan, China, where he is currently working toward the Ph.D. degree in optical engineering. His research focuses on the algorithm and application of distributed acoustic sensing.

Hao Li received the B.S. degree in 2017 in optoelectronics information science and engineering from the Huazhong University of Science and Technology, Wuhan, China, where he is currently working toward the Ph.D. degree in optical engineering. His research focuses on high sensitivity and high-SNR distributed acoustic sensing.

Tao He received the B.S. degree in optical information technology from Wuhan Textile University, Wuhan, China, in 2016, and the master's degree in 2019 from the Huazhong University of Science and Technology, Wuhan, China, where he is currently working toward the Ph.D. degree in application security. His research focuses on machine learning based on distributed fiber sensor.

Shixiong Zhang received the B.S. degree in electronic information engineering from the Wuhan University of Science and Technology, Wuhan, China, in 2019, and the master's degree in 2021 from the Huazhong University of Science and Technology, Wuhan, China, where he is currently working toward the Ph.D. degree in application security. His research focuses on machine learning based on distributed fiber sensor.

Baoqiang Yan received the B.S. degree in optical information technology from Nanchang Hangkong University, Nanchang, China, in 2016 and the master's degree from the Taiyuan University of Science and Technology, Taiyuan, China, in 2020. He is currently working toward the Ph.D. degree in optical engineering with the Huazhong University of Science and Technology, Wuhan, China. His research focuses on distributed acoustic sensing.

Zhijun Yan received the B.S. and master's degrees in condensed matter physics from Lanzhou University, Lanzhou, China, in 2003 and 2006, respectively, and the Ph.D. degree in optoelectronics from Aston University, Birmingham, U.K. He was engaged in the design of novel fiber optic devices, theoretical and preparative technologies, fiber optic sensors, and fiber lasers. He has already established strong background for the theoretical research and fabrication technique of tilted fiber grating.

Qizhen Sun (Senior Member, IEEE) received the B.S. and Ph.D. degrees from the Huazhong University of Science and Technology,Wuhan, China, in 2003 and 2008, respectively. In 2015, she was promoted to a Full Professor of optoeletronics with the School of Optical and Electronic Information, Huazhong University of Science and Technology. She is widely authored or coauthored in the leading scholarly journals, invited to giving talks on international conferences and workshops, authorized 36 patents, and also dedicated to promote the industrial applications of the developed sensors. Her research interests include micro/nano-structured fiber optical devices, optical fiber sensing technologies and applications. Prof. Qizhen Sun was granted the Marie Curie Fellowship of the European Union in 2013, the Excellent Young Scientist of China in 2019, and also has been a Senior Member of since 2017.